Journal of Techniques, ISSN: 2708-8383, Vol. 6, No. 4, 2024, Pages 57-72
DOI: https://doi.org/10.51173/jt.v6i4.2472

JOURNAL OF TECHNIQUES

Journal homepage: http://journal.mtu.edu.iq

RESEARCH ARTICLE - MECHANICAL ENGINEERING

Redesign the Best Model for Lower Link Arm in the MF Tractor by Finite Element Analysis

Tariq Mahmoud Chliab[1], Ali Adelkhani[1*]

[1]Department of Mechanical Engineering, Kermanshah Branch, Islamic Azad University, Kermanshah, Iran

[*] Corresponding author E-mail: a.adelkhani@iauksh.ac.ir

Article Info.

Article history:

Received
05 March 2024

Accepted
12 September 2024

Publishing
31 December 2024

Abstract

The lower link arm of the tractor is one of the parts that are exposed to heavy static, dynamic, and fatigue loads. If the lower link arm is damaged, the agricultural operations will be stopped and the machinery connected to it will also be damaged. Therefore, it is necessary to design this arm so that it is resistant to various loads. This article redesigns and analyzes the MF Extra 290 tractor's lower link arm in response to plowing power. SolidWorks software was used to design different arm models, and stress was analyzed using Abaqus software. Nine different arm models were designed with three different cross-sectional shapes (Rectangular-Narrow Center) and three volume methods (Straight, Vertical Convex, and Horizontal Convex). The best arm model, according to the results, is an extruded one with a rectangle-shaped, wide center. The safety factor for this model of the arm is 1.82. In all arm models, maximum stress was observed in the hole connecting the lower arm to the hydraulic jack of the tractor.

Publisher: Middle Technical University

Keywords: Tractor; Arm; Design; Stress; Von Miss.

1. Introduction

Several studies have been conducted as a result of ongoing attempts to improve agricultural machinery, and it is important to pay attention to every facet of this problem. Using computer-aided design approaches, it is now possible to investigate elements including forces, stress distribution, deformations, and how to best optimize the performance of components and structures [1,2]. Before creating the initial prototype, the finite element method (FEM) is a rapid and accurate computational technique used to analyze stress, strain, and deformation in mechanical components, as well as to pinpoint critical and non-critical areas. Through the modification of valuable characteristics, such as the materials and surface conditions. This method leads to analysis in a virtual environment without the need for a physical model [3, 4].

One of the most significant and essential agricultural implements is an off-road tractor. The majority of agricultural sectors use it. The tractor's power and the large range of attachments and implements it can tow or push allow it to be used for a variety of purposes. The tractor, which is the most significant piece of agricultural machinery, plays a major role in the mechanization of planting, retaining, and harvesting operations. Therefore, in order to achieve sustainable agriculture and improve the level of mechanization, it is necessary to attain the highest level of manufacturing technology for this agricultural machinery as well as its quantity [5, 6].

One of the most well-known agricultural machineries is the farm tractor, which utilizes a three-point hitch system for lifting, pulling, and other field chores. Due to heavy operating loads, one of the main issues with tractors is the lower arms or lower link breaking or deforming at the attachment points to agricultural tools. Because of this, the lower arms are among the most important three-point hitch components in tractors. If this component fails, attached implements may be damaged, resulting in financial losses and injuries to farmers. Therefore, it would appear that in order to determine the root cause of failure or shape of deformation, a mechanical examination of the lower arms of tractors operating under the most demanding conditions is required.

Agricultural machinery has a lot of moving parts which work under large static and dynamic loads, which can cause failure and downtime. One of the parts of tractors that are exposed to heavy static, dynamic and fatigue loads, is the lower link arm which puts a lot of load on it and makes it break easily. If the lower link arm is damaged, agricultural operations will stop, and the tools and machinery connected to it will also be damaged. Therefore, it is necessary to design this arm to have a high resistance to various loads. Therefore, in this research, this arm was redesigned and was analyzed under the influence due to plowing operation force to select the most suitable model.

Finding safety factors under static stress during field service was the goal of this work, which aimed to analyze the lower arm of a three-point hitch of a tractor using the finite element technique. The findings of this research may be utilized to make conclusions about the requirement for optimization, mechanical strength, and material behavior in the tractor's lower arms [7-11].

Nomenclature & Symbols			
FEM	Finite Element Method	FS	Factor Safety
MPa	Mega Paskal	SF	Strength Factor
FEA	Finite Element Analysis	N	Newtons Unit
CAD	Computer Aided Design	KN	Kilo Newton Unit

The main contributions of this research focus on the relationship between the dependent variables the von Mises stress and the arm displacement and the independent variables the dimensions and geometric characteristics of the lower link. Previous research has not addressed the innovative focus of changing the lower link arm of the widely used Massey Ferguson XTRA 290 tractor in Iraq, which is the main contribution of this study. Using Finite Element Analysis (FEA), this study is the first to examine the effects of varying the lower link arm's geometric parameters on the stress distribution within the component. We show that adjusting the geometric dimensions makes it possible to select a design with higher strength and stress resistance while simultaneously lowering the maximum stress that the arm can endure. Using calipers and rulers, the researchers precisely measured the measurements of the tractor arm. Then, they studied various agricultural operations to determine which put the most strain on the arm. The next step was to use SolidWorks to create the arm model and then Abaqus for analysis. We found the best design and determined how much stress each model could withstand by doing these analyses.

The main objective of this research is to design a new lower link arm to withstand more load and stress than the current arm of the tractor under study.

Other sub-objectives are:

- Finding effective parameters in stress distribution in the lower link arm performing
- Stress analysis in different designed models
- Design a new model to withstand more load.

This manuscript is structured as follows: Section 2 discusses the recent research. Section 3 discusses the finite element analysis. Section 4 describes the types of FEA software. Section 5 discusses the tractor and the three-point hitch. Section 6 discusses the experimental data. Section 7 shows the software implementation. Section 8 describes the analysis under four different loading conditions and the results. Section 9 describes the conclusions.

2. Related Work

The Finite Element Method (FEM) is being used more and more to tackle intricate engineering problems in agricultural machinery. This is because the components of these machines often experience significant static and dynamic stresses, which can result in possible failures. Researchers have been able to examine, optimize, and enhance many components and systems of agricultural equipment by applying Finite Element Method (FEM) in this discipline. Initial applications of Finite Element Method (FEM) in agriculture involve analysing the stress levels in crucial components like the mouldboard Plow and disk Plow. For example, [12] performed stress analysis on a mouldboard Plow, whereas [13] examined the pressures exerted on a disk Plow in real-world field settings. Subsequent research broadened the application of Finite Element Method (FEM) to more essential elements. Stress and fatigue analysis using Finite Element Method (FEM) was conducted on the connecting rod of MF-285 and Universal 650 tractors' engines, which identified the areas with the maximum concentration of stress. Researchers have investigated mower pulleys, spur gears, and front axles of combine harvesters. One study, referenced as [14], discovered a low safety factor in the front axle of the JD 955 combine harvester. In addition, study [15] investigated the causes of failure in the position axle of a tracked tractor, while study [16] analysed fatigue fractures in the rear axle of a tractor, offering valuable information for enhancing material and design.

The Finite Element Method (FEM) has been applied in the mechanical analysis and optimization of three-point hitch components. These components are essential for the functioning of tractors in field duties, such as lifting and hauling. A study [17] examined the performance of a subsoil blade in a non-uniform sandy-loam soil, showcasing the efficacy of Finite Element Method (FEM) in simulating and evaluating tillage equipment. In addition, a study was undertaken by [18] to dynamically optimize the design of a subsoiler to improve its fatigue resistance. [19] and [13] examined the mechanical strain and soil deformation caused by rotating tiller blades on different soil compositions in the broader context. Additional finite element method (FEM) simulations were performed on several components, including the front axle and straw walker cranks of JD combine harvesters, lift arms of three-point hitch tractors, and vibration analysis of a chopper's pulley.

The lower arms of tractors, an essential component of the three-point hitch system, are especially susceptible to failure when subjected to heavy workloads. The significance of mechanical inspections of these components has been emphasized by research conducted at the Institute of Agricultural Machinery of the Technical University of Munich [20] and other institutions [21, 22]. The Finite Element Method (FEM) was employed to examine the safety factors and natural frequencies of the lower arms of MF399 and MF285 tractors when subjected to static stresses. The research indicated that optimization is required to improve mechanical strength and material properties. It was also proposed that either the lifting capacity should be restricted or the design and manufacturing process of the lift arms should be modified to avoid failures.

Recent progress has also involved utilizing optimization tools, such as Altair Hyper Works, to develop crucial components, such as the check chain mounting bracket, for Mahindra tractors. [23] such tools can enhance dimensions, save material expenses, and enhance machinery dependability. This compiled section lays the groundwork for future developments in the sector by offering a thorough review of the substantial contributions FEM has made to bettering the design, analysis, and optimization of components of agricultural machinery.

3. Finite Element Analysis

Engineering problems that would be challenging to answer using analytical techniques can be solved numerically using finite element analysis (FEA). Calculating stresses, deflections, and displacements in both simple and complex structures is one of its primary applications. The use of FEA in thermal, structural, and fluid flow analysis has also been expanded (see Fig. 1). The essential philosophy is the same even though it is applied to numerous engineering domains [24].

The structure or component being analysed is essentially split into manageable, manipulable bits. According to Logan, this procedure is known as discretization, and the finite element method entails modelling the structure using tiny, interconnected elements known as finite elements, each of which is associated with a displacement function. Then, through shared or common interfaces, such as nodes, boundary lines, and/or surfaces, these elements are connected to every other element directly or indirectly [25].

- The behaviour of a given node in terms of the qualities of every other element in the structure is then ascertained using the material's known stress and strain properties that make up the structure. Each node's version of these is made into an equation, and matrices can be used to solve the entire set of equations to determine how the structure will behave overall. Matrices are simpler to compare than the challenging differential equations that come from analytical analysis. By increasing the number of nodes, the numerical method can achieve a better estimated result, but this obviously leads to an even larger set of equations. This type of equation can be solved using the computer's computational capability, according to the underlying theory of the FEA software [26]. Finite Element Analysis is used to:
- It is employed as a low-cost method of ensuring that a new design or a change to an already-existing structure or component will fulfill the necessary structural, modal, or thermal standards. The traditional method of manufacturing, which entails designing, creating a prototype, and conducting field testing, is costly since the structural behavior of the new design cannot be determined until it has undergone field testing. Any further issues with the new design could necessitate the costly redesign and modification of the prototype. Finite Element Analysis eliminates the requirement to construct a prototype for testing. The new model is tested and adjusted as necessary before the part is made or constructed. Effectively, FEA is a cost-cutting exercise. It is possible to predict a component's behaviour before it is manufactured, avoiding the need to create a prototype that might fall short of expectations [27].
- The components are loaded and restricted in accordance with actual circumstances. The model can be subjected to loads through the use of finite element analysis. To simulate real-world situations where components can be fixed in different translations or may be attached using a pin joint that enables rotation, constraints like displacements, planar constraints, and pin constraints can also be employed [28].
- Depending on the complexity of the component and the computer's capabilities, the results showing how the component will act under the specified loadings and limitations can be processed quickly. If the outcomes of an analysis are unsatisfactory, the shape of a model can be simply changed [28].
- It is possible to trust the results of a finite element analysis. This is based on the analyst's level of expertise. The software can yield results that are pretty respectable when used properly. [29] carried out an experiment to test the accuracy of the conclusions drawn from a finite element analysis. They came to the conclusion that there was a 5.17% difference between the experiment's results and those of the finite element analysis. The difficulty, however, lies in interpreting the FEA findings and ensuring that the loadings and constraints have been applied correctly to a well-prepared model. [28] asserts that the calibre of the supplied data affects the outcomes of a FEA modelling. When utilizing a FEA package, according to the component in the upper left corner of the Fig. 2 has a rough mesh that has been improved in (b) and (c) by adding more nodes and components (see Fig. 2). In (a), the nodes are symbolized by a few dots, and the element is the line that connects them [29].
- The ability to quickly change the model shape is another benefit of creating 3D parametric models and using them for FEA. The analyst can easily modify the geometry in the 3D model by changing the governing parameters if the FEA findings are considered unacceptable [27].

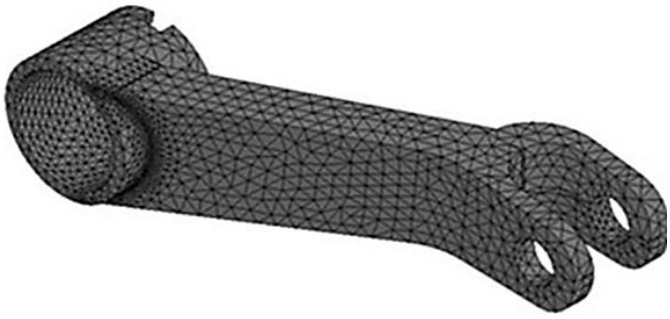

Fig. 1. Finite element analysis of lift arm of a MF-285 tractor [22]

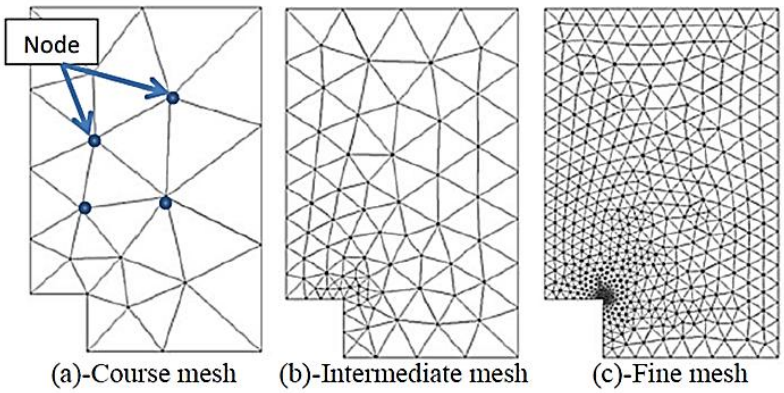

Fig. 2. Mesh refinements [29]

4. Types of FEA Software (Basic Steps of FEA)

There are many different FEA software programs available, and they differ in terms of their features, cost, and usability. Some free software has constrained functionality; for instance, FELIPE can only carry out four functionalities out of a possible twenty-three. Despite being gratis, some software includes advanced features. Elmer, for example, can execute about 15 of the twenty-three potential functions. Even though a package is premium software, it may not always have more features than certain gratis. When determining which FEA package to utilize, one should take into account the package's capabilities to carry out the particular application in question. Applications include thermal, computational fluid dynamics, static and structural analysis, and many others. Finding expensive software that have very few uses is not unusual. These are intended for specialized uses including fluid flow analysis and the design of civil and structural systems. ADINA, ANSYS Mechanical NEi/Nastran, Pro/MECHANICA Wildfire 2, COSMOS Works, COMSOL, and Strand 7 are the most used packages in the business and have a wide range of capabilities [30].

4.1. Grid quantities

The extent of the computing workload and the precision of the computations are directly impacted by the number of grids. Accuracy can be increased by using more grids; however, doing so increases the computational load. When the number of grids is minimal, adding more grids will dramatically increase accuracy without significantly increasing the amount of computation. When the number of grids reaches a certain point, adding more grids won't have much of an impact on the accuracy of the final calculation but will result in a significant rise in processing volume. Therefore, when choosing the number of grids, accuracy and computation volume should both be considered [31].

4.2. Unit type

The accuracy of the results is highly tied to how to select the right unit type. Rod units can only support pressure or pushing forces directed at the rod; they are not capable of supporting bending moments. Both tensile and bending moments can be handled by the beam unit. The shell element is best suited for constructions with thin walls, which can somewhat lessen the computational complexity. The common hexahedral elements, which are frequently utilized for straightforward structural analysis, have higher calculation power than the solid components. A tetrahedral unit with an intermediary node is an excellent option for complex constructions [31].

4.3. Meshing

The process of meshing, which approximates the solution domain as a discrete domain made up of finite units of various sizes, is known as meshing. One of the most important and challenging problems in this procedure is how to distribute the model among the right number of cells. Higher accuracy is correlated with smaller grids, but calculations become more complex. We should employ a denser grid to imitate the data change law in the situation of stress concentration, or when the data change ladder is larger. On the other hand, we should increase the evacuation network if the gradient of change is small to lighten the workload [32].

4.4. Unit order

The units come in three different shapes: linear, quadratic, and cubic; the latter two are referred to as higher order units. The unit's high-order form provides a greater precision advantage. It typically utilizes a high-order unit because its surface or surface boundary can fit the surface or surface boundary of the examined structure when evaluating a more complex or non-uniform stress distribution structure. The number of grids and nodes will, however, substantially increase as a result of the related use of high-order units. Therefore, the unit order needs to be balanced to take time consumption and accuracy into account. It will employ multiple unit orders in the unified structure in order to optimize the software because increasing the number of grids or the unit order can significantly improve the calculation's accuracy. We shall choose a high-order unit if the structure is complicated or the stress is concentrated, and a low-order unit if the results must have low accuracy. Unit form, or the shape of the grid's individual elements, is crucial to the accuracy of the calculations and can potentially cause them to fail [33].

5. Tractor and the Three-Point Hitch

A common form of hitch for connecting ploughs and other implements to an agricultural or industrial tractor is the three-point hitch (British English: three-point linkage). Either a triangle or the letter A can be seen as the three points. The only method of attaching two bodies in engineering that is statically determined is three-point attachment. When an implement is connected to a tractor using a three-point hitch, its orientation in relation to the tractor and the hitch's arm position is fixed. All or part of the weight of the implement is carried by the tractor as Fig. 3. The drawbar, a single point, pivoting connection when the implement or trailer is not in a fixed position with respect to the tractor, is the other primary method for attaching a load [34].

Harry Ferguson invented the three-point hitch in the 1920s as a standard way to fasten implements (equipment) to tractors. A rigid connection is created by the three-point hitch's employment of one upper and two lower attachment points. The lower arms' lower hydraulic cylinders elevate and lower the implement. The top arm may be affected by a second hydraulic arm to adjust the draft (depth) of tillage equipment. The three-point hitch's ability to translate the equipment's drag into a downward push on the tractor's rear is a considerable benefit. This indicates that when pulling is most challenging, traction is at its greatest [35].

The three-point hitch is made up of a number of interconnected parts. These include the lifting arms, stabilizers, attachment points, and the tractor's hydraulic system. Three movable arms make up three-point hitches. The hydraulic system controls the two lower arms, known as the hitch lifting arms, which lift, lower, and even tilt the arms. The top link, the upper center arm, can move but is often not propelled by the tractor's hydraulic system. There is an attachment on each arm that allows you to attach tools to the hitch. The implements have posts that fit through the attachment holes in each hitch, allowing for the attachment of the implements. A pin is used to fasten the device by going through the ends of the posts [36]. The tractor's internal hydraulic system provides power to the hitch raising arms. The operator controls the hydraulic system, and often a number of settings are offered. Modern three-point hitch systems frequently have a draft control device. The hydraulic system automatically raises the arms slightly when the draft increases and lowers them when the draft falls based on the amount of force required to draw the implement, which is sensed on the top link [37].

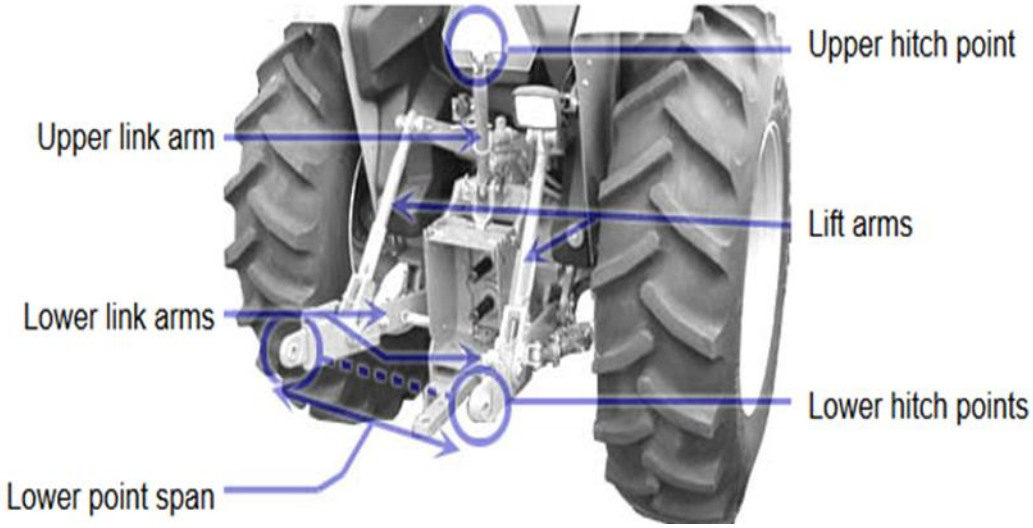

Fig. 3. Different components of the three-point connection of the tractor and the position of the lower arm [37]

6. Experimental Data

One of the biggest issues in engineering is mechanical breakdown of machine parts. [38] employed ANSYS finite element software for stress analysis under both static and dynamic situations and CATIA mechanical software to simulate the tractor-operated rotary blades, offering the best possible design. See Fig. 4. His study's end objective was to provide a model for the blades' mechanical behavior and the magnitude of the forces operating on them in the field. [39] used CAD (computer aided design) software for structural analysis and computer aided engineering analysis to design a rotary tillage equipment based on FEM and simulation methods. Fig. 5 depicts the rotary mower's deformation and stress plot.

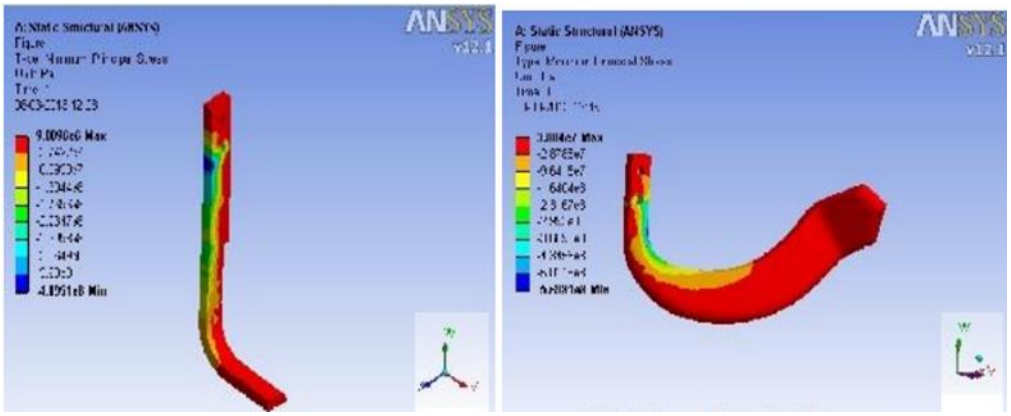

Fig. 4. Rotary weedier blades Analysis [38]

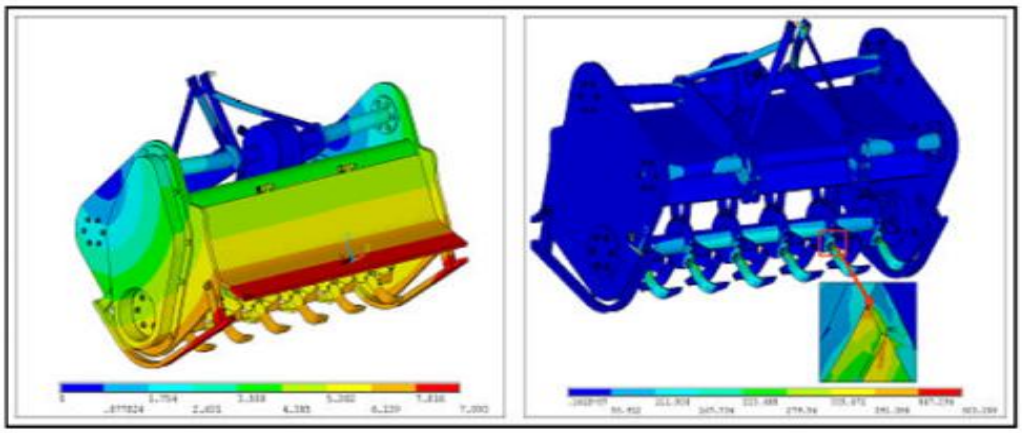

Fig. 5. Deformation and stress plot for rotary mower [39]

W. Yingkuan [40] evaluated the Factor of Safety (FS) of the garden tractor's hybrid aluminium composite rear axle using the FEM. For FEA modeling, they employed the CATIA and ANSYS software. The findings showed that under dynamic loading circumstances, composites had a greater fatigue strength factor (SF) than an unreinforced alloy. Additionally, the outcomes demonstrated that composite materials have a higher SF at maximum static loading. The rear axle of a garden tractor's maximum von Mises stress and displacement are shown in Fig. 6.

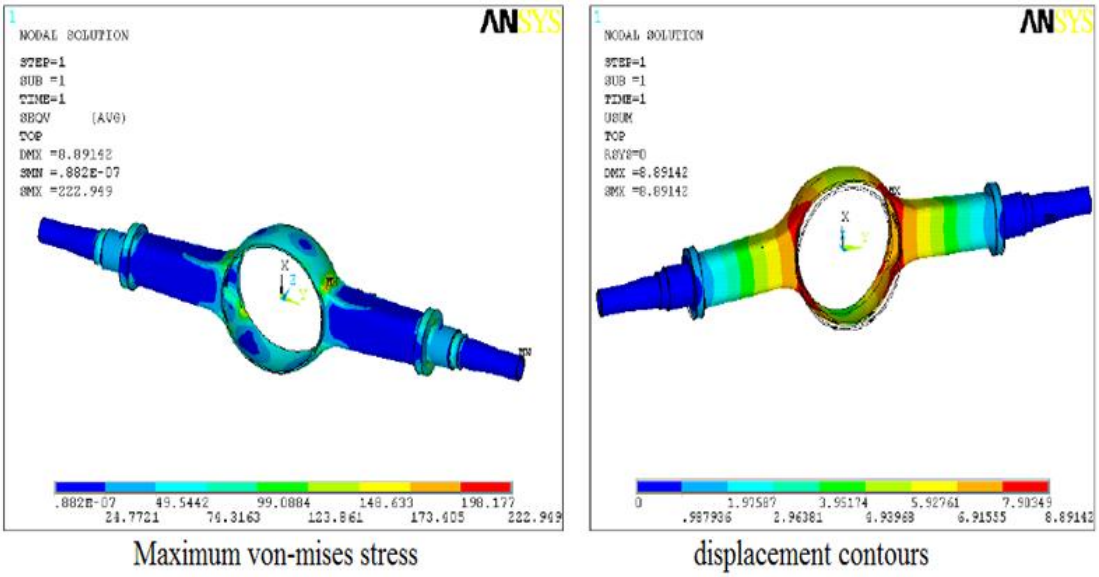

Fig. 6. Maximum Von Mises stress and displacement of rear axle of garden tractor [40]

Using the finite element approach, [41] determined the maximum stresses in the connecting rod of the tractor (MF-285) engine. In this study, the total forces applied to the connecting rod were estimated in order to determine its stress. The connecting rod was then modelled, meshed, and imported into the ANSYS 9 program. The pin end and rod couplings as well as the bearing cup and connecting rod linkage experienced the highest-pressure stress. The lower part of the pin end and the connections between the pin end and the rod obtained the highest tensile stress. Another similar study for the dynamic analysis of a mini tractor crankshaft was conducted by [42]. This investigation helped to determine the crankshaft's fatigue life shown in Fig. 7. To gain a better knowledge of the mechanical behaviour of the crankshaft in dynamic conditions, they applied the modal analysis method.

In a different study, 3D models of shredder parts were created using Pro/Engineer software, as shown in Fig. 8. They put the essential components of this device together with the aid of the same software before performing finite element analysis on them.

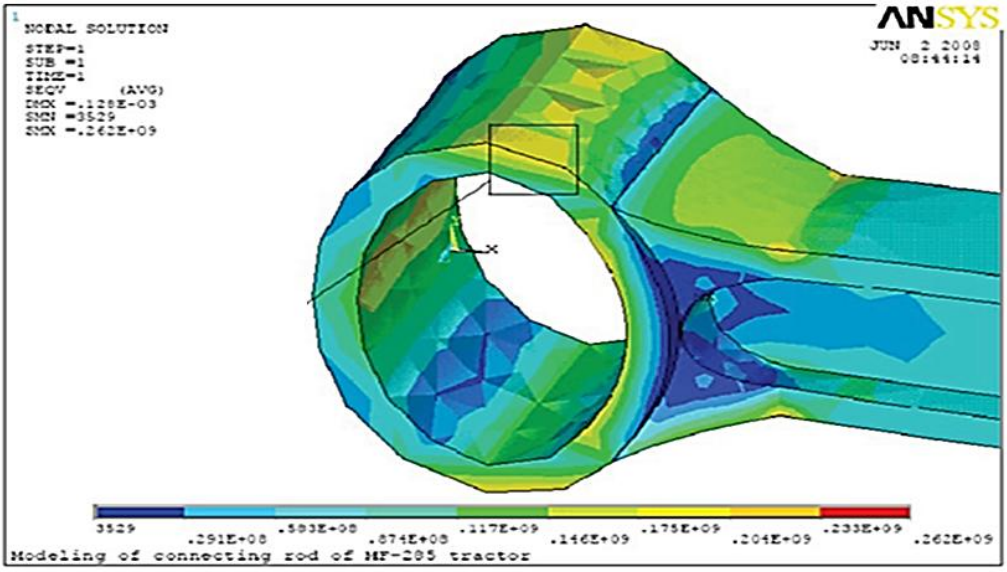

Fig. 7. Stress distribution in the pin end, resulting from maximum tensile force considering Von Mises [41]

7. Software Implementation

Computer-aided design software and computer-aided analysis software were both used in this work, as seen in Fig. 9. The initial modeling of several arms was done in this work using SolidWorks, one of the most well-liked CAD programs. SolidWorks is a tool for modeling solids that is based on the Parasolid kernel and builds models and assemblies using feature-based parametrics. Nine distinct lower arm models were created

for this study. Compared to comparable CAD programs like CATIA, Pro/Engineer, Unigraphics, Mechanical Desktop, and Inventor, SolidWorks has unique characteristics that set it apart:

- Usability and ease compared to other CAD software in design and training.
- Faster than other software, in comparison.
- The capacity to carry out engineering analysis by putting the parameters to use in a very user-friendly and straightforward way.
- Communication skills with all machining and analytical software.

After a piece has been created using CAD software, CAE software must engineer and analyze the piece's structural makeup. Abaqus was utilized in this study to model the operating conditions for the arms and analyze the pressure. The core concept of the software was outlined in David Hibbitt's Brown University dissertation from 1972, titled Computational Mechanics Based on the Finite Element. The flexibility of Abaqus, as opposed to other finite element programs now on the market, is one of its most significant advantages, shown in Fig. 10. Subroutine programming, a feature that accomplishes this, is a very potent tool for professional users. A user-written Fortran subroutine is a group of code created for a particular application. One can define new behavioral models, apply unique loads, and perform other functions using this capability. The two software's environments are displayed in Fig. 10.

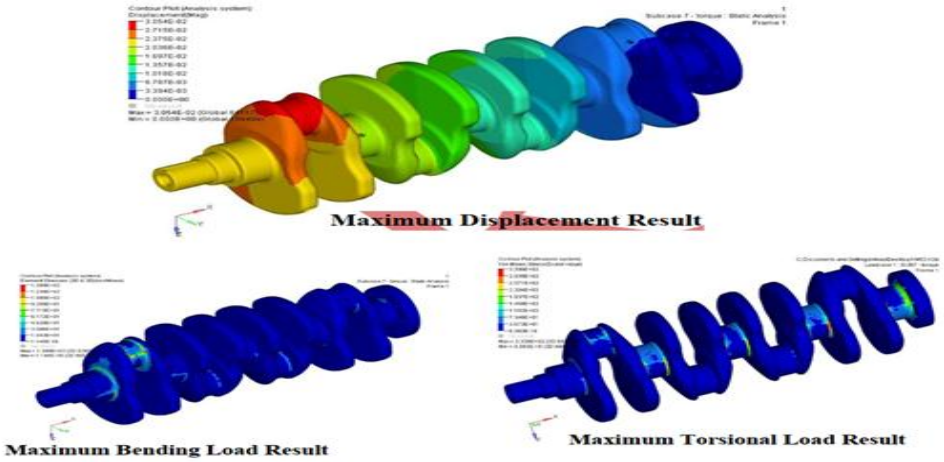

Fig. 8. Maximum displacement, bending, and torsional results in the crankshaft [42]

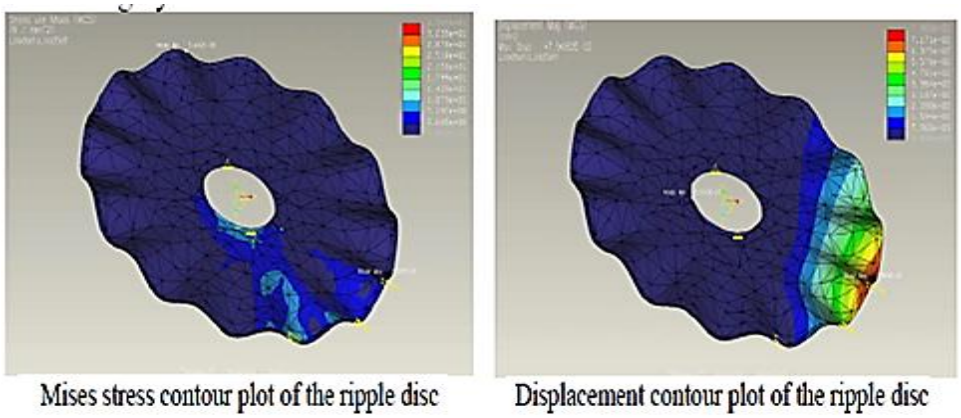

Fig. 9. Stress analysis in disc blades

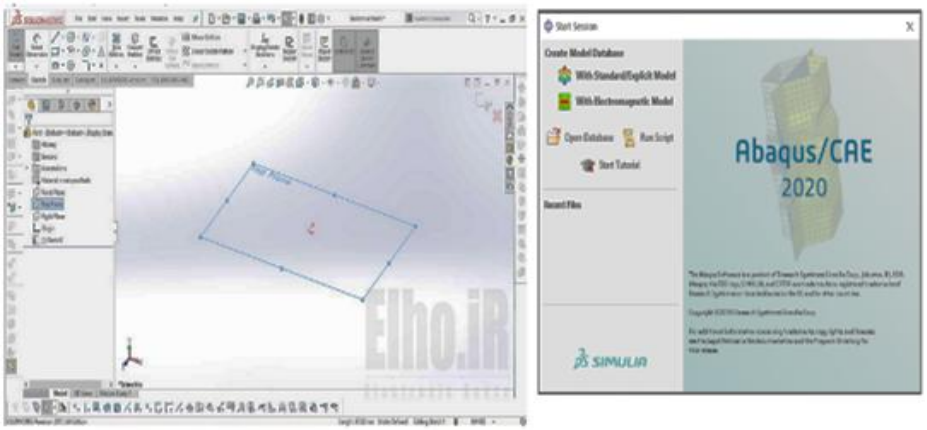

Fig. 10. SolidWorks and Abaqus environment

7.1. The studied tractor

One of the most popular models of tractor in Iraq is the Massey Ferguson Xtra 290. Details about the tractor are shown in Table 1. This tractor is utilized for plowing and disking in difficult agricultural tasks. One component that will break during demanding agricultural work is the lower arm of the tractor. In order to find a model that can withstand higher pressure, it must be optimized and redesigned. Fig. 11 depicts the lower link arm of the tractor as well as the jack's dimensions and size, the transverse motion control cable, and other details shown in Table 1. To ensure that the position of the arms with respect to one another is implemented as standard, the end ball of the arm, which is attached to the tractor chassis, was constructed with a 16-degree angle.

Table 1. Specifications of the studied tractor

Properties	Unit	Amount
Model	--	Massey Ferguson 290 Xtra
Weight	kg	3010
Power	hp	81.8
Drawbar Power	hpN.m	53.32
Torque		291

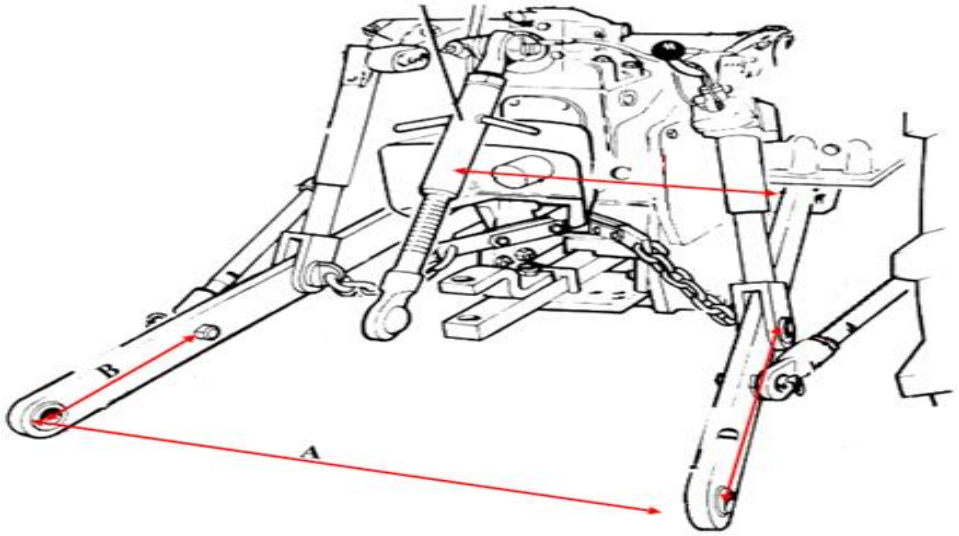

Fig. 11. Dimensions and size of the end position of the tractor's lower arm (A: 100 cm, B: 39 cm, C: 39 cm, D: 63 cm)

7.2. Designed arms

For the MF Xtra 290 tractor, nine lower arm versions were created for this study. The first model of the tractor arm was created via manual measurement; see Table 2. The model was square-shaped. Fig. 12 depicts the model's size and dimensions. The arm was altered to strengthen its construction and bear additional pressure. Two more models for the lower arm were created for this study. It should be emphasized that all created models' biggest cross sections, 20 cm^2, were regarded as equal. The models were made in the same sizes as well. The models of various arms and their specifications are displayed in Table 2.

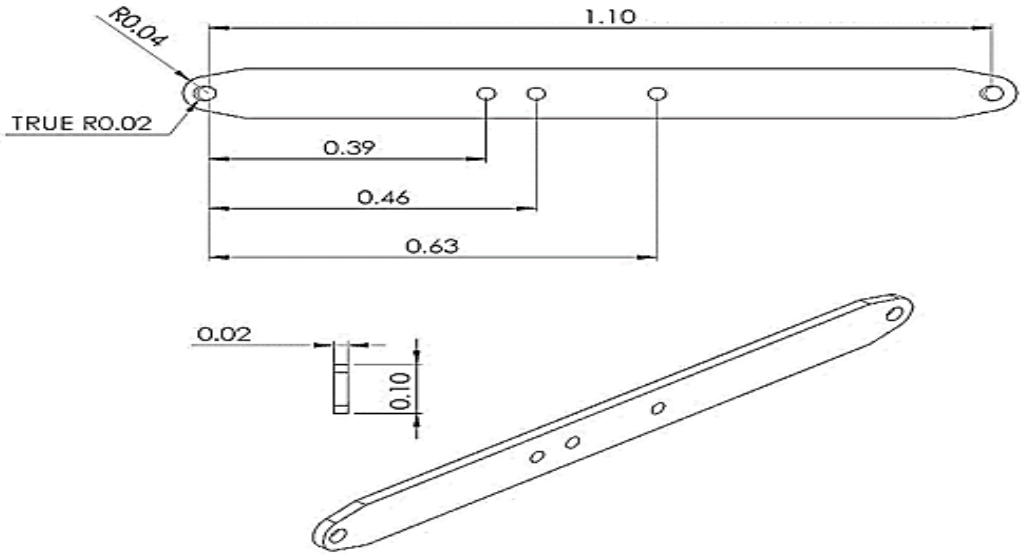

Fig. 12. Dimensions in (m) and size of the tractor's main arm

Table 2. Specifications of different models designed for the lower arm

Model Number	Cross section shape	Cross-sectional volume method
1	Rectangle	Straight Vertical Convex Horizontal Convex
2	Rectangle (Narrow Center)	Straight Vertical Convex Horizontal Convex
3	Rectangle (Fat Center)	Cross-Section Convex

As illustrated in Fig. 13, the rectangular cross-section, the wide-center rectangular cross-section, and the narrow-center rectangular cross-section were all taken into consideration for the arm. The cross section of the arms was developed initially, followed by the volume or extrude section, which employed three techniques: straight extrude, vertical convex extrude, and horizontal convex. The various arm configurations for the rectangular wide-center cross section are shown in Fig. 14.

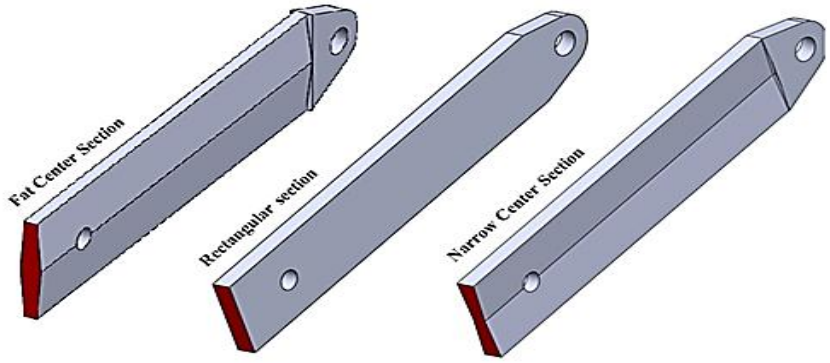

Fig. 13. Different cross sections designed for the lower arm

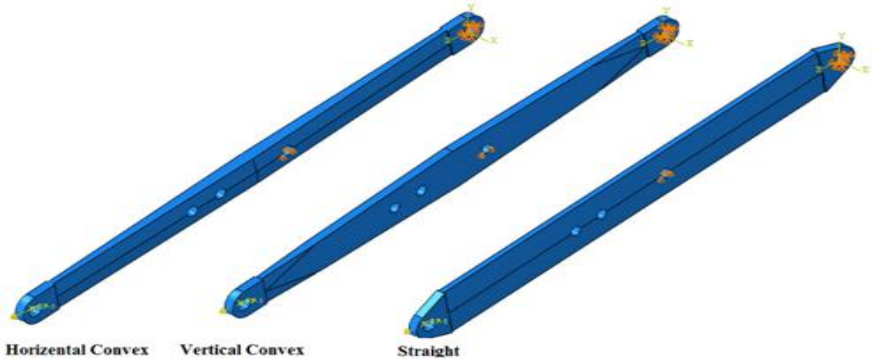

Fig. 14. Different forms of extrusion of the tractor's lower arm

7.3. Finite element analysis

Without employing an approximation, the analytical solution uses mathematical concepts to solve an equation over the entire problem space. A mathematical equation that contains well-known mathematical operators and functions can be used to solve a closed problem. The numerical solution approach is a strategy for approximate problem-solving using a limited vocabulary of mathematical expressions. The Rayleigh-Ritz approach, the finite element method, the boundary element method, the discrete element method, the finite difference method, and the network-less methods are the numerical solution techniques most frequently employed in stress analysis. In this work, the pressurized tank's stress and stress behavior were examined using the finite element method. The finite element method is a numerical method for estimating solutions to boundary value problems in engineering. One or more dependent variables must satisfy a differential equation at every point in a specified domain of independent variables (often a physical structure) for the boundary value problem to exist mathematically. Field variables, such as physical displacement, temperature, heat flux, and fluid velocity, are dependent variables that are controlled by the differential equation of the problem Fig. 15. Specific values of field variables (or associated variables like derivatives) at field boundaries are known as boundary conditions.

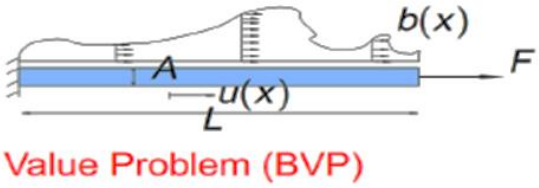

Fig. 15. Boundary value problem

7.4. Model entry in abaqus

The SolidWorks arm models were imported into the Abaqus environment. To do this, the created models were exported in.x-t format and then imported into the Abaqus environment. The arm's physical and mechanical parameters were initially entered into Abaqus after the model was imported, in accordance with Table 3, and the properties were then allocated to the tractor arm.

Table 3. Specifications and physical and mechanical properties of ASTM-A36 steel

Material	Steel	ASTM-A36
Density	7860	Kg/m^3
Ultimate strength	400	MPa
Yield Strength	250	MPa
Modulus of Elasticity	200	GPa
Modulus of Rigidity	77.2	GPa

7.5. Applying force and determining the boundary conditions of the problem

The tractor arm is subjected to tensile and flexural loads depending on the working conditions. In this study, first, the maximum tensile force in the tractor arm was measured according to Equation 1:

$$F = \frac{P}{V} \quad (1)$$

In Equation 1, P, F, and V are the tractor mounting power in watts (W), the force on the tractor arms in Newton (N), and the tractor advancing speed in meters per second (m/sec), respectively. According to research conducted by [42], the best and most appropriate tractor speed for plowing with a reversible plow is 2.458 km/h (0.6828 m/s). Based on this result, it was assumed that the tractor should work at the same speed in the field, for which the amount of force created in the tractor arm was measured according to Equation 2:

$$F = \frac{39.78kW}{0.6828\frac{m}{s}} = 58.26\ kN \quad (2)$$

Based on the above-mentioned relationships, it was discovered that during the plowing process using the reverse plow at the optimum speed, the maximum force on each of the lower arms reached 58.26 kN, and was distributed between the arms. However, this force is directed to the lower arm in different directions depending on the plowing depth and changing working conditions. Accordingly, the applied force was studied in this research at four different angles: 0, 5, 10, and 15 degrees with respect to the horizontal surface. Fig. 16 shows the position of the load applied to the arm and the location of the lower arm supports. Point C was identified as the place where the load was directed to the lower arm of the tractor. The angle of the force relative to the horizontal direction and its value are shown in Table 4.

Table 4 The amount and direction of force on the lower arm

Angle of force relative to the horizon line (degrees)	Fz (kN)	Fy (kN)
0	29.264	0
5	29.152	-2.55
10	28.82	-5.08
15	28.26	-7.57

Fig. 16 defines the restraint method for the lower arm. At the junction of the lower arm to the main chassis (A), the arm was restrained in three directions x, y, and z. At point B, which is where the lower arm connects to the arm of the hydraulic jack, movement in the direction of the y-axis was restrained. In general, and in terms of torque, the arm was not restrained in any direction.

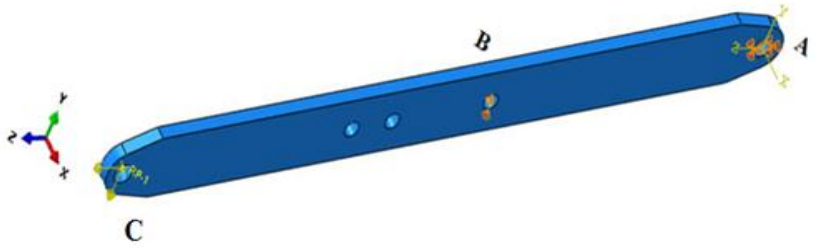

Fig. 16. The location of the load on the arm and the location of the lower arm supports

7.6. Selecting the type of the element

A complex mathematical problem can be solved by the finite element method with correct recognition of the nature of the problem and the prevailing mathematical relations. In so doing, after selecting the appropriate solver, the elements should be considered the most important factor in solving a problem in finite components. Selecting the correct type of element, network size, and a number of integration points directly affects the convergence of the solution and achieves the desired answer. Gridding or meshing algorithm refers to a set of techniques for creating a network of regular and practical finite elements on a geometric model. It is interesting to know that these methods are dependent on the shape of the element (types of element shapes in Abaqus) and the meshing technique, and depending on the type of network selected, the user is given several options. This study used a tetrahedral element. Fig. 17 shows the type of selected element in Abaqus.

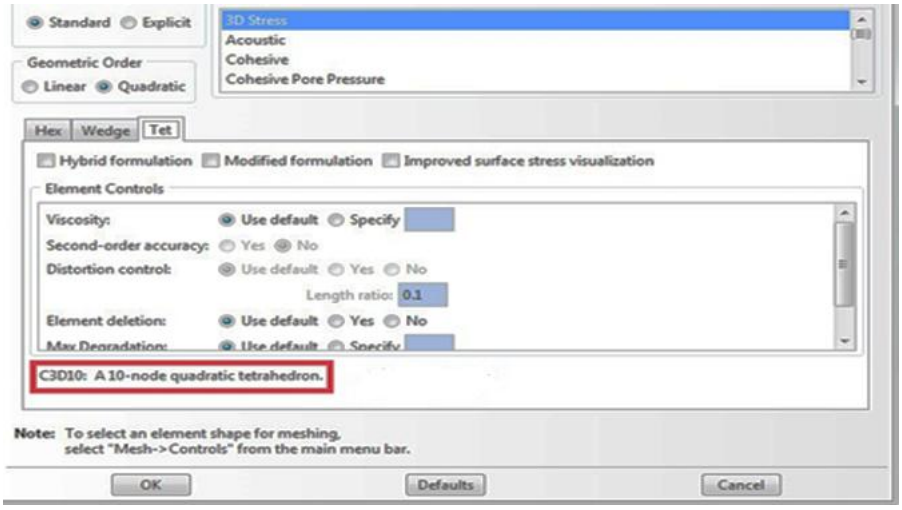

Fig. 17. Selecting a tetrahedral element

7.7. Model meshing

The solutions derived to solve a problem using the finite element method show that the convergence of the numerical solution is always contingent on both the mesh size and the size of the elements utilized. When you augment the mesh density, meaning you decrease the dimensions of the elements and, consequently, reduce the volume of the elements, the numerical solution of the problem tends to approach a singular solution. However, the smaller the mesh, the greater the hardware power used to solve the finite element model, and the more time the processing takes. If through successive reduction of the size of the elements, negligible changes in the results of the solution are obtained, it is said that the mesh has converged. In this study, before solving the problem, the convergence process was performed to select the optimal mesh size. Fig. 18 shows the meshing manner in the components of the arm. The mesh size around the arm holes was smaller than elsewhere.

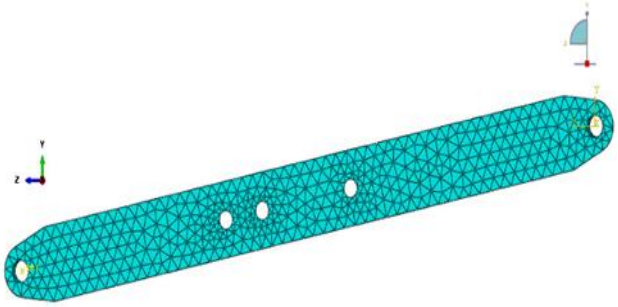

Fig. 18. The meshing manner of the arm

7.8. Analysis of results and stress criterion

In the structure, failure basically occurs in stress points. In other words, parts of the structure that have low stress or strain have little effect on the strength of the structure. In an ideal structure, the stress is the same at all points and close to a safe value. Accordingly, waste in the structure can be removed. The stress level in the element is obtained by comparing Von Mises stress of that element with the maximum or average value of this stress in the whole structure. Accordingly, in this study, Von Mises stress model was used to analyze the results [42].

8. Analysis in Four Different Loading Conditions

Due to the dependence of the finite element solution results on the mesh size used, the mesh convergence should always be checked in areas of the model where the values of stress, strain, contact pressure, or any other parameter should be accurately and intelligently measured so as not to cause a sharp increase in computational volume. The solution to a problem depends on the size of the elements used. If the results do not change significantly as the size of the elements decreases, the mesh is said to have converged. Therefore, in this study, for the number of different elements in Abacus, changes in the maximum Von Mises stress in the pressurized tank were investigated. These changes are shown in Fig. 19. As shown in Fig. 19, the maximum amount of Von Mises stress increased with increasing the number of elements under the same loading conditions. When the number of elements was 2800, the changes in maximum stress were almost constant, and the slope of the diagram line was nearly zero, which indicated that as the number of elements increased, there was no change in the end result. The tractor's lower arm exhibited Von Mises stress. Thus, in order to reduce the computation time and eliminate the effect of the number of elements on the output results of Abacus, the number of mesh elements for the present study was considered in the range of 2800-3000 elements.

8.1. Stress analysis in the initial model of the lower arm of the MF Xtra 290 tractor

In this section, the results of the analysis of 9 arm models and 4 different loading conditions are presented. In total, the maximum stress was measured for 36 models. Fig. 20 shows the maximum Von Mises stress for different methods of extruding the lower arm and different directions of force for the wide-centre rectangular arm. For all forces on the arm, the maximum Von Mises stress was observed in the lateral convex or horizontal convex extrusion method. In most loading conditions, the minimum Von Mises stress was observed in the straight extrusion mode.

Moreover, the study of the effect of force on the lower arm showed that when the force was zero degrees relative to the arm, the maximum observations of Von Mises stress were made, , and the Von Mises stress was found to be at its lowest when the angle between the force and the arm was 10 degrees. Fig. 21 displays the key stress distribution states in the lower arm for three distinct arm extrusion procedures. The area where the maximum Von Mises stress was observed was at the connection of the hydraulic jack handle to the lower arm. For all three extrusion methods, the stress distribution was as shown in Fig. 21, only the amount was different.

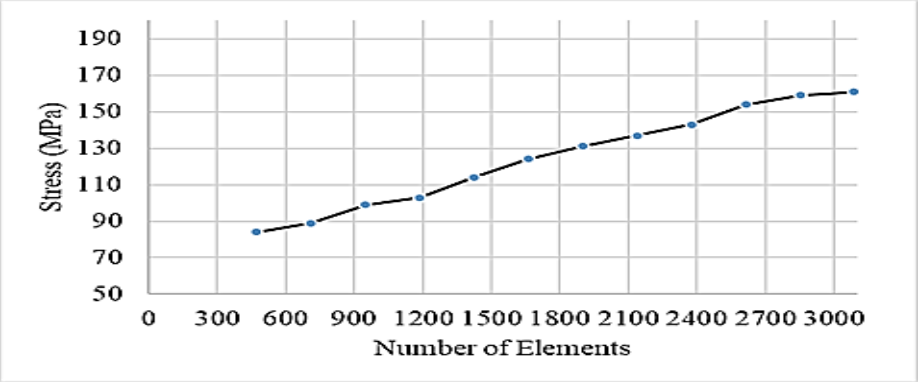

Fig. 19. Maximum Von Mises stress changes in the tank for the number of different elements

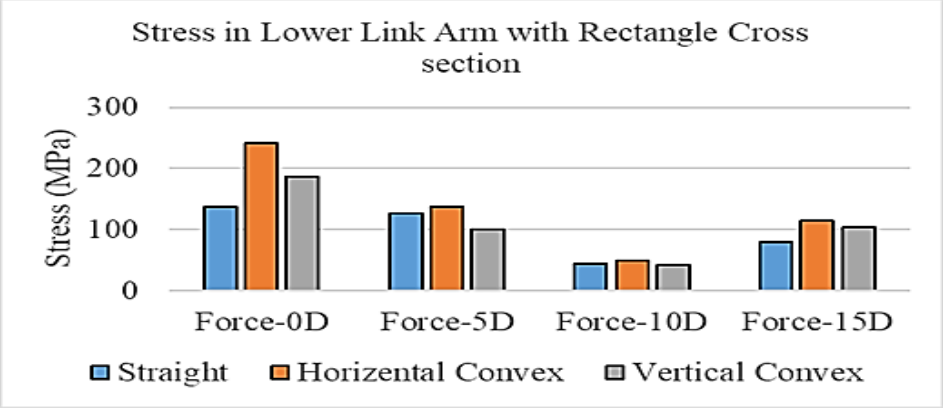

Fig. 20. Maximum Von Mises stress in wide-center rectangle arm for different directions of force

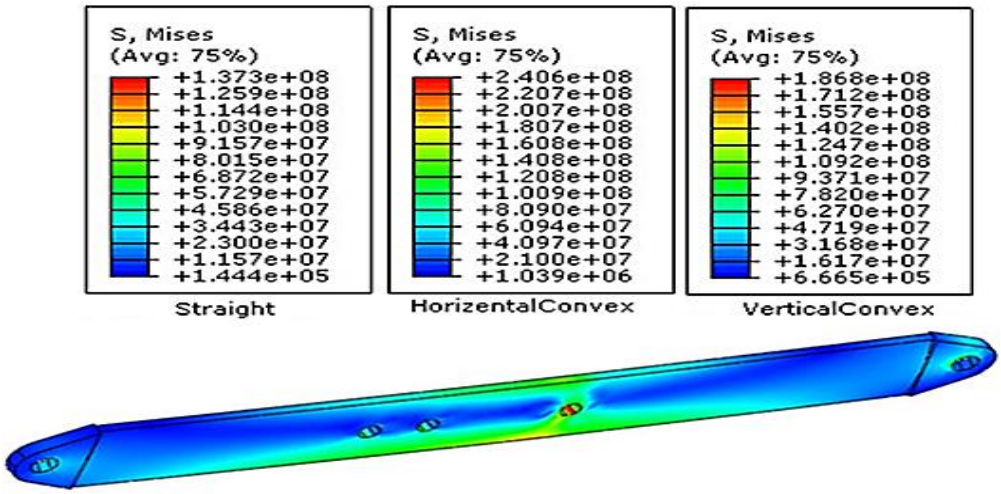

Fig. 21. Stress distribution in the lower arm with a wide-center rectangular cross-section for different methods of arm extrusion (angle between the force and the arm was zero degrees)

The results of this section showed that the best way to build a lower arm with a wide-center rectangular cross-section was to maintain the uniformity of the cross-section along the entire length of the arm. At the same time, if the arm is positioned so that the direction of the tensile force and the arm make an angle of 10 degrees with one another, in this case, the minimum tension is obtained in the lower arm. As the results show, the maximum Von Mises stress was observed in the wide-center rectangular section arm that was 240.6 MPa. The reliability coefficient for this case was approximately 1.04. However, the most optimal design mode for the arm with a wide-center rectangular cross-section was obtained in the straight extrusion mode, which was assumed to have a maximum force of 1.8 on the arm.

8.2. Stress analysis in the arm with a narrow-center rectangular cross-section

Fig. 22 shows the maximum stress observed in the arm with a narrow-center rectangular cross-section for different loading conditions and different arm extrusion methods. The maximum Von Mises stress was observed for all three models of arm extrusion where the angle between the force and the arm was zero degrees. In this case, the maximum stress for the extruded conditions of the arm in the straight, vertical convex, and horizontal convex conditions were 154.7, 260.4, and 186 MPa, respectively. By altering the force direction while keeping the force magnitude constant at 29.3 kN, it was observed that the minimum stress occurred when the angle between the force and the arm was 10 degrees. However, as the angle between the force and the arm increased, the maximum stress also increased. In Fig. 23, one can see the stress distribution in the lower arm with a narrow-center rectangular cross-section for various methods of arm extrusion when the force and the arm were aligned at a zero-degree angle. As in the previous section, the results indicated that the highest Von Mises stress was situated at the junction where the lower arm connected to the tractor hydraulic jack. The most optimal design configuration for the arm with a narrow-center rectangular cross-section was achieved in the straight extrusion mode. Assuming the maximum force was applied to the arm, the reliability value for this model was 1.62.

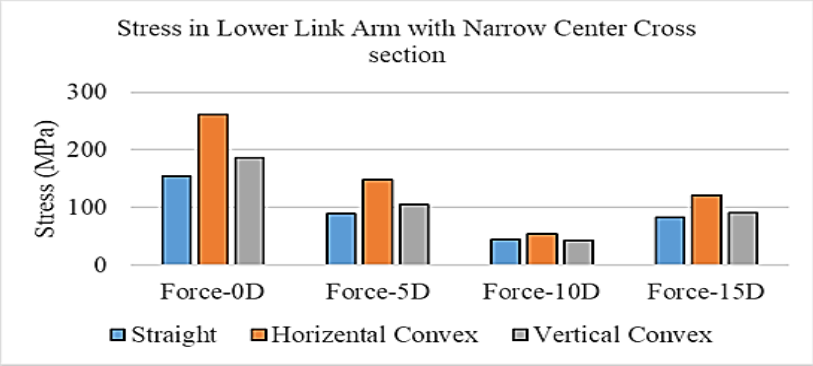

Fig. 22. Maximum Von Mises stress in the narrow center section arm for different directions of force

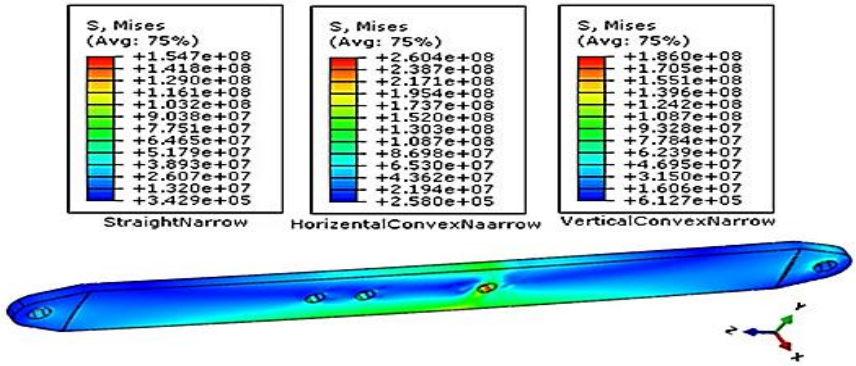

Fig. 23. Stress distribution in the lower arm with a narrow-center rectangular cross-section for different methods of arm extrusion (angle between the force and the arm was zero degrees)

8.3. Stress analysis in the arm with rectangular cross section

Fig. 24 shows the maximum Von Mises stress in the arm with a center rectangular cross-section for different directions of force. In this section, like the previous sections, the maximum Von Mises stress was observed when the direction of the force and arm was parallel. Furthermore, the lowest Von Mises stress was observed in all different loading modes in straight extrusion mode. The minimum Von Mises stress was observed when the angle between the force and the arm was 10 degrees Fig. 25 shows the distribution and amount of stress in the arm for different forms of arm extrusion. The maximum Von Mises stress was observed in the lower arm, and the reliability coefficient for the straight rectangular arm extrusion was 1.56.

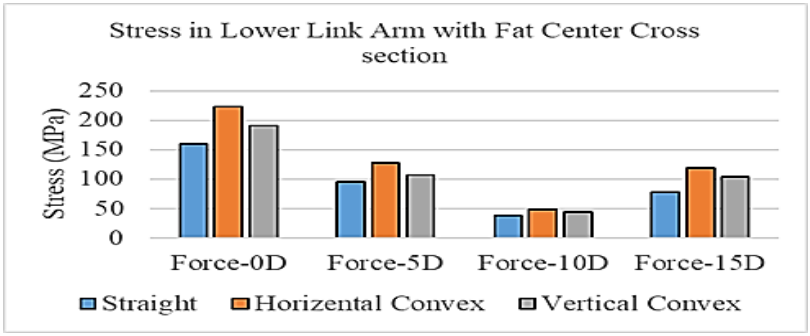

Fig. 24. Maximum Von Mises stress in rectangle arm for different directions of force

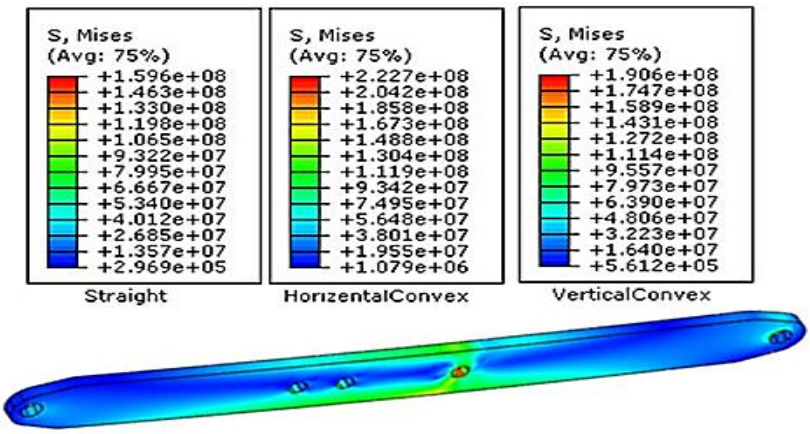

Fig. 25. Stress distribution in the lower arm with rectangular cross-section for different methods of arm extrusion (angle between the force and the arm was zero degrees)

In general, the results of the stress analysis showed that the maximum stress created in the arm changed with alterations in the cross-section and extrusion method of the lower arm of the tractor. Assuming a fixed arm cross section, the minimum Von Mises stress was observed in the arm designed by the straight extrusion method and the maximum stress for extruded arm by the horizontal convex method. In general, when the cross section was given a uniform volume, the stress distribution in the arm was uniform and the focus area was less stressed, thus the stress in this form was less than the arm. Additionally, the area where the maximum stress was observed was the same in all different forms of the arm, which was observed in the context of junction where the lower arm meets the tractor hydraulic jack. The results of this section showed that if the traction force of the tractor and the lower arm is zero degrees, in this case, the maximum Von Mises stress would be created in the arm, which would decrease and then increase with increased angle. For an angle of 10 degrees, the minimum tension in the lower arm was observed for all the studied modes. However, it is necessary to consider the fact that the force applied to the tractor arm does not have a fixed direction because during agricultural operations, the tensile force direction and the lower arm would change with changing the plowing depth. Thus, the arm should be analyzed where the Von Mises stress is maximum, which in this study was the most critical case when the angle between the arm and the force is zero degrees. The following is the result of the change in the arm length only for a zero-degree angle of tensile force and the arm. Fig. 26 compares the maximum stress in different models of designed arms and shows that the best model for the lowest Von Mises stress was the wide-center rectangular cross-section of the straight extrusion, for which the reliability coefficient of the arm was 1.82.

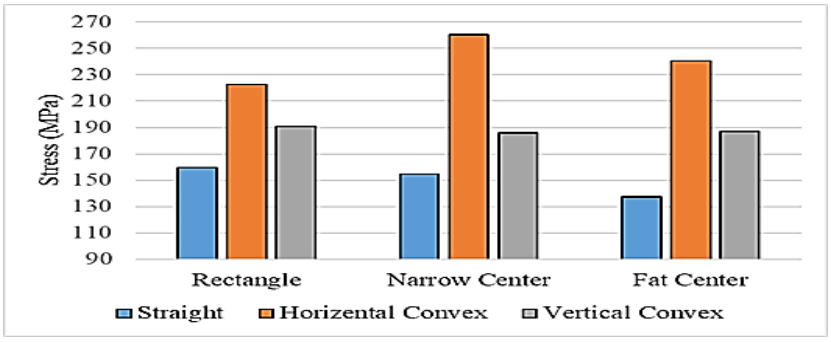

Fig. 26. Comparison of maximum stress in different models of designed arm

The analysis of the displacement in the arm is shown in Fig. 27, which depicts the maximum displacement value in different models of the designed arm. The results showed that the minimum displacement and relocation were observed in the arm with a wide-center rectangular cross section and straight extrusion method. Fig. 28 shows the displacement distribution for this model of the arm. The maximum displacement was observed at the junction of the arm to agricultural tools. In other words, the maximum displacement occurred at the point where the load was applied in general, the displacement analysis of the designed arms was similar to the stress analysis, and the results showed that the best arm model for minimizing displacement involved changing the length of the wide-center rectangular arm using the straight extrusion method.

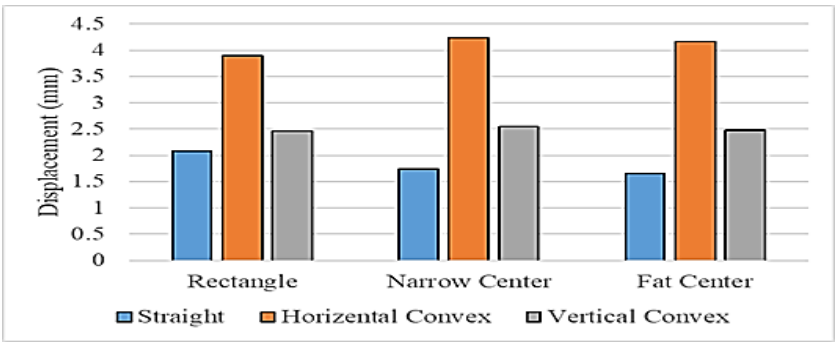

Fig. 27. Comparison of maximum displacement in different models of designed arm

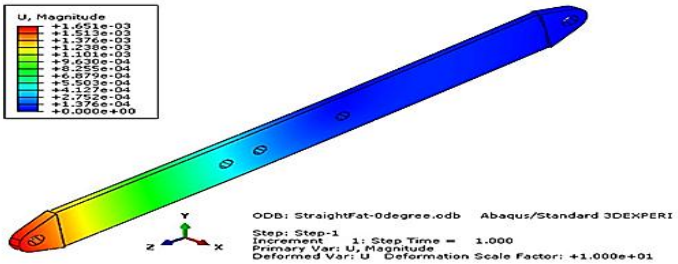

Fig. 28. Displacement distribution along the tractor's lower arm

9. Concussion

In this study, 9 models were designed for the tractor's lower arm, and the effect of tensile force on stress distribution and maximum displacement in each arm model was investigated. By changing the cross-section and extrusion method of the tractor's lower arm, the maximum tension created in the arm was changed. Assuming the arm cross section constant, the minimum Von Mises stress was observed in the arm designed by the straight extrusion method and the maximum stress for extruded arm by horizontal convex method. The point where the maximum stress was observed in all forms of the arm was the same and occurred at the connection between the arm and the tractor's hydraulic jack When the tractor's tensile force direction of the lower arm was at zero degrees, the maximum Von Mises stress was observed in the arm, which would decrease and then increase with an increasing angle. For a 10-degree angle, the lowest tension in the lower arm was observed for all the studied modes. The most critical point was when the angle between the arm and the force was zero degrees. The best model for the lowest Von Mises stress arm was the wide-canter rectangular cross section of the straight extrusion, which had a reliability coefficient of 1.82 for this model of arm. The maximum displacement was created at the application point of the load. The best arm model for the minimum displacement was to change the length of the wide-canter rectangular arm by the straight extrusion. In future work, we suggest that the arm be analyzed under dynamic loading, the optimal arm shape of this model be made and installed on a tractor in a laboratory with the available sample and their function be compared, design a system on the tractor that always adjusts the position of the tractor's lower arm so that the tensile force direction and the tractor arm are at 10 degrees, and propose that in a separate study, the location of the arm connection to the hydraulic jack be redesigned to reduce the concentration of stress in that area.

Acknowledgement

We would like to thank the head of the Department of Mechanical Engineering and all the department's teaching staff for their assistance.

References

[1] M. Wozniak, A. Rylski, and K. Siczek, "The Measurement of the Wear of Tie Rod End Components," Strojniški vestnik - Journal of Mechanical Engineering, vol. 68, no. 2, pp. 101–125, Feb. 2022, doi: 10.5545/sv-jme.2021.7389.
[2] R. Barbieri and N. Barbieri, "Finite element acoustic simulation-based shape optimization of a muffler," Applied Acoustics, vol. 67, no. 4, pp. 346–357, Apr. 2006, doi: 10.1016/j.apacoust.2005.06.007.
[3] L. Wang, P. K. Basu, and J. P. Leiva, "Automobile body reinforcement by finite element optimization," Finite Elements in Analysis and Design, vol. 40, no. 8, pp. 879–893, May 2004, doi: 10.1016/s0168-874x(03)00118-5.
[4] A. Janulevičius and V. Damanauskas, "How to select air pressures in the tires of MFWD (mechanical front-wheel drive) tractor to minimize fuel consumption for the case of reasonable wheel slip," Energy, vol. 90, pp. 691–700, Oct. 2015, doi: 10.1016/j.energy.2015.07.099.
[5] E. C. R. McKenzie et al., "Versatile Tools for Understanding Electrosynthetic Mechanisms," Chemical Reviews, vol. 122, no. 3, pp. 3292–3335, Dec. 2021, doi: 10.1021/acs.chemrev.1c00471.
[6] F. Williamson, "Richard courant and the finite element method: A further look," Historia Mathematica, vol. 7, no. 4, pp. 369–378, Nov. 1980, doi: 10.1016/0315-0860(80)90001-4.
[7] W. Riedel, "Beiträge zur Lösung des ebenen Problems eines elastischen Körpers mittels der Airyschen Spannungsfunktion," ZAMM - Journal of Applied Mathematics and Mechanics / Zeitschrift für Angewandte Mathematik und Mechanik, vol. 7, no. 3, pp. 169–188, Jan. 1927, doi: 10.1002/zamm.19270070302.
[8] O. Kohnehpooshi and M. S. Jaafar, "Non-Linear Three Dimensional Finite Elements for Composite Concrete Structures," Latin American Journal of Solids and Structures, vol. 14, no. 3, pp. 398–421, Mar. 2017, doi: 10.1590/1679-78253170.
[9] A. Kurniawan and Andoko, "Stress and Crack Simulation on Axle Housing Mitsubishi L300 Pickup Car using Finite Element Method," IOP Conference Series: Materials Science and Engineering, vol. 494, p. 012107, Mar. 2019, doi: 10.1088/1757-899x/494/1/012107.
[10] B. Fellah, N. Cherif, M. Abri, and H. Badaoui, "CSRR-DGS Bandpass Filter Based on Half Mode Substrate Integrated Waveguide for X-Band Applications," Advanced Electromagnetics, vol. 10, no. 3, pp. 39–42, Nov. 2021, doi: 10.7716/aem.v10i3.1782.
[11] M. Abbaspour-Gilandeh, G. Shahgoli, Y. Abbaspour-Gilandeh, M. A. Herrera-Miranda, J. L. Hernández-Hernández, and I. Herrera-Miranda, "Measuring and Comparing Forces Acting on Moldboard Plow and Para-Plow with Wing to Replace Moldboard Plow with Para-Plow for Tillage and Modeling It Using Adaptive Neuro-Fuzzy Interface System (ANFIS)," Agriculture, vol. 10, no. 12, p. 633, Dec. 2020, doi: 10.3390/agriculture10120633.
[12] A. Hemmat, N. Nankali, and N. Aghilinategh, "Simulating stress–sinkage under a plate sinkage test using a viscoelastic 2D axisymmetric finite element soil model," Soil and Tillage Research, vol. 118, pp. 107–116, Jan. 2012, doi: 10.1016/j.still.2011.10.016.
[13] D. P D, S. K M, and A. K K, "Investigation on Static Stress Analysis of Portal Axle Gearbox," International Journal of Applied Engineering Research, vol. 13, no. 07, p. 5244, Apr. 2018, doi: 10.37622/ijaer/13.7.2018.5244-5250.
[14] H. K. Celik, N. Caglayan, M. Topakci, A. E. W. Rennie, and I. Akinci, "Strength-based design analysis of a Para-Plow tillage tool,"

Computers and Electronics in Agriculture, vol. 169, p. 105168, Feb. 2020, doi: 10.1016/j.compag.2019.105168.
[15] G. Suresh Kumar and L. A. Kumaraswamidhas, "Design optimization focused on failures during developmental testing of the fabricated rear-axle housing," Engineering Failure Analysis, vol. 120, p. 104999, Feb. 2021, doi: 10.1016/j.engfailanal.2020.104999.
[16] K. Tamás, I. J. Jóri, and A. M. Mouazen, "Modelling soil–sweep interaction with discrete element method," Soil and Tillage Research, vol. 134, pp. 223–231, Nov. 2013, doi: 10.1016/j.still.2013.09.001.
[17] E. Ebrahimi and K. Mollazade, "Intelligent fault classification of a tractor starter motor using vibration monitoring and an adaptive neuro-fuzzy inference system," Insight - Non-Destructive Testing and Condition Monitoring, vol. 52, no. 10, pp. 561–566, Oct. 2010, doi: 10.1784/insi.2010.52.10.561.
[18] S. Rooppakhun and K. Siamuna, "Finite Element Analysis of Dynamic Hip Screw for Intertrochanteric Fracture," International Journal of Modeling and Optimization, pp. 158–161, 2012, doi: 10.7763/ijmo.2012.v2.103.
[19] İ. Yavuz, "FAILURE ANALYSIS OF A TRACTOR FRONT AXLE," Materiali in tehnologije, vol. 57, no. 2, Mar. 2023, doi: 10.17222/mit.2022.711.
[20] A. Y. K. Chung, N. Qamaruz Zaman, F. Y. Abd. Manaf, R. Mohamed Halim, and R. Abd. Majid, "Palm Oil Mills Odour Emission Survey based on Different POME Treatment Systems," Jurnal Kejuruteraan, vol. 33, no. 1, pp. 113–131, Feb. 2021, doi: 10.17576/jkukm-2021-33(1)-12.
[21] E. Seyedabadi, "Finite Element Analysis of Lift Arm of a MF-285 Tractor Three-Point Hitch," Journal of Failure Analysis and Prevention, vol. 15, no. 5, pp. 737–743, Sep. 2015, doi: 10.1007/s11668-015-0010-0.
[22] D. G. Spear, A. N. Palazotto, and R. A. Kemnitz, "Modeling and Simulation Techniques Used in High Strain Rate Projectile Impact," Mathematics, vol. 9, no. 3, p. 274, Jan. 2021, doi: 10.3390/math9030274.
[23] P. Wriggers, "Nonlinear finite element analysis of solids and structures," European Journal of Mechanics - A/Solids, vol. 17, no. 6, p. 1044, Jan. 1998, doi: 10.1016/s0997-7538(98)90517-4.
[24] M. M. Islam, J. A. Epaarachchi, and H. Su, "Vinyl Ester/Glass Microballoon Syntactic Foams with Low Density," International Research Journal of Materials Sciences and Applications, pp. 1–25, 2017, doi: 10.28933/ijmsa-2017-01-01.
[25] J. Mosely, "SMPTE Tutorial Paper: Computerized Tracing of Magnetically Striped Theatrical Release Prints," SMPTE Journal, vol. 93, no. 11, pp. 1057–1061, Nov. 1984, doi: 10.5594/j16838.
[26] A. Kujansivu and J.-Å. Rosell, "Complex Instruction as a tool for developing the role of the teacher. A workshop presented at the 'Intercultural Education and Co-operative Learning' conference in Ghent, May 2000," Intercultural Education, vol. 11, no. sup1, pp. 21–26, Dec. 2000, doi: 10.1080/14675980020010836.
[27] Fialko, S. and Karpilovskyi, V., 2018. Time history analysis formulation in SCAD FEA software. Journal of Measurements in Engineering, 6(4), pp.173-180, doi.org/10.21595/jme.2018.20408
[28] M. Hillman and J.-S. Chen, "An accelerated, convergent, and stable nodal integration in Galerkin meshfree methods for linear and nonlinear mechanics," International Journal for Numerical Methods in Engineering, vol. 107, no. 7, pp. 603–630, Dec. 2015, doi: 10.1002/nme.5183.
[29] K. Berzina, I. Zicmane, T. Lomane, and S. Gusev, "Theoretical Aspects of Risk Assessment in Power Supply System Operation," International Journal of Electrical Energy, vol. 7, no. 2, pp. 44–50, Dec. 2019, doi: 10.18178/ijoee.7.2.44-50.
[30] K. IWATA and Y. YAMADA, "Nonlinear Structural Stability Analysis by the Finite Element Method," Transactions of the Japan Society of Mechanical Engineers, vol. 42, no. 354, pp. 444–452, 1976, doi: 10.1299/kikai1938.42.444.
[31] H.K., Yilmaz, D., Ünal, N. and Akinci, I., 2009. Failure analysis of a location axle in a tracked tractor. Journal of Failure Analysis and Prevention, 9(3), pp.282-287, doi.org/10.1007/s11668-009-9232-3
[32] Ľ. Hujo, Z. Tkáč, J. Tulík, J. Kosiba, D. Uhrinová, and M. Jánošová, "Monitoring of operation loading of three-point linkage during ploughing," Research in Agricultural Engineering, vol. 62, no. 1, pp. 24–29, Mar. 2016, doi: 10.17221/10/2015-rae.
[33] G. Molari, M. Mattetti, and M. Walker, "Field performance of an agricultural tractor fitted with rubber tracks on a low trafficable soil," Journal of Agricultural Engineering, vol. 46, no. 4, p. 162, Dec. 2015, doi: 10.4081/jae.2015.477.
[34] D. C. Scholtz, "A three-point linkage dynamometer for restrained linkages," Journal of Agricultural Engineering Research, vol. 11, no. 1, pp. 33–37, Mar. 1966, doi: 10.1016/s0021-8634(66)80006-9.
[35] A. Veludurthi and V. Bolleddu, "Evaluation of Small Wind Turbine Blades with Uni-Vinyl Foam AlignmentsUsing Static Structural Analysis," Energy Engineering, vol. 117, no. 4, pp. 237–248, 2020, doi: 10.32604/ee.2020.011304.
[36] G. U. Shinde and S. R. Kajale, "Design Optimization in Rotary Tillage Tool System Components by Computer Aided Engineering Analysis," International Journal of Environmental Science and Development, pp. 279–282, 2012, doi: 10.7763/ijesd.2012.v3.231.
[37] M. A. Zamora, "Petrographic microscopy of geologic textural patterns and element-mineral associations with novel image analysis methods," May 30, 2024. https://doi.org/10.5204/thesis.eprints.248815.
[38] X. Yaoyang and W. J. Boeing, "Mapping biofuel field: A bibliometric evaluation of research output," Renewable and Sustainable Energy Reviews, vol. 28, pp. 82–91, Dec. 2013, doi: 10.1016/j.rser.2013.07.027.
[39] F. H. Montazersadgh and A. Fatemi, "Optimization of a Forged Steel Crankshaft Subject to Dynamic Loading," SAE International Journal of Materials and Manufacturing, vol. 1, no. 1, pp. 211–217, Apr. 2008, doi: 10.4271/2008-01-0432.
[40] W. Yingkuan, "Editorial Team of International Journal of Agricultural and Biological Engineering," International Journal of Agricultural and Biological Engineering, vol. 7, no. 5, pp. 1–6, Oct. 2014, doi: 10.3965/ijabe.v7i5.1538.
[41] M. Xiao, J. Zhao, Y. Wang, H. Zhang, Z. Lu, and W. Wei, "Fuel economy of multiple conditions self-adaptive tractors with hydro-mechanical CVT," International Journal of Agricultural and Biological Engineering, vol. 11, no. 3, pp. 102–109, Jan. 2018, doi: 10.25165/j.ijabe.20181103.2158.
[42] N. D. Lagaros, M. Papadrakakis, and G. Kokossalakis, "Structural optimization using evolutionary algorithms," Computers & Structures, vol. 80, no. 7–8, pp. 571–589, Mar. 2002, doi: 10.1016/s0045-7949(02)00027-5.